An amphiphilic C_{60} penta-addition derivative as a new U-type molecular rectifier

Sandhyarani Acharya, Hyunwook Song, Jongman Lee, Pil Sook Kwon, Jung-pil Lee, Gottikunda Yogendranath, Young Ha Kim, Yun Hee Jang, Takhee Lee, Shashadhar Samal *, Jae-Suk Lee *

Department of Materials Science and Engineering, Gwangju Institute of Science and Technology(GIST), 261 Cheomdan-gwagiro (Oryong-dong), Buk-gu, Gwangju 500-712, Republic of Korea

ARTICLE INFO

ABSTRACT

Unimolecular rectification behavior of a known amphiphilic fullerene derivative, 1,4,11,15,30-pentakis(4-hydroxyphenyl)-2H-1,2,4,11,15,30-hexahydro-[60]fullerene, (4-$HOC_6H_4)_5HC_{60}$ (referred to here as the fullerene pentapod), is reported. The HOMO and LUMO energy levels of the pentapod were determined by density functional theory calculations (B3LYP/6-31G**). It was found that the HOMO of the donor moiety and the LUMO of the acceptor are in the same fullerene cage, quite unlike the fullerene derivatives so far reported as molecular rectifiers. The molecule formed a stable Langmuir-Blodgett film at the air–water interface. Characterization of the film indicated that it constitutes mostly a monolayer of molecules with the hydrophobic C_{60} moiety pointing upwards. The LB film was transferred over Au(1 1 1) substrate and electrical conductivity of the film was measured by conducting atomic force microscopy. An asymmetric electrical rectification behavior was observed in the voltage range of ±1.0 V to ±2.0 V. Beyond a bias voltage of ±2.0 V, rectification ratio decreased steadily, until at ±2.5 V the current–voltage curve became symmetric. The observed electrical rectification behavior was ascribed to resonant electron tunneling between the Fermi level of the electrode and the molecular orbital levels of the fullerene pentapod. Charge transport in the preferred direction under a suitable applied bias was facilitated due to efficient electronic interactions of the molecular orbitals through a combined effect of homo- and peri-conjugation. This constitutes a new class of donor–acceptor system and a step forward in the field of molecular electronics.

© 2008 Published by Elsevier B.V.

1. Introduction

Stable molecular diodes neatly arranged without defects are a viable answer to continued quest for ultimate device miniaturization in electronics [1,2]. The possibility that a single molecule could function as a rectifier was proposed by Aviram and Ratner with an exemplary theory of rectification [3]. This initial theory, modified subsequently [4], led to a wide interest in the field of unimolecular rectification for over a decade [5]. 'Unimolecular rectification' is a conventional terminology, which in reality concerns the rectification behavior of an ordered assembly of molecules, since isolating and probing the electrical behavior of a single molecule is rather impractical. A number of systematic studies have been devoted to understand the rectification behavior of an organized array of molecules in Langmuir-Blodgett (LB) films, or self-assembled monolayers (SAM) of organic molecules. The molecules invariably contained an electron donor moiety (D) bound to an electron acceptor (A) through an insulating saturated σ- or

* Corresponding authors. Tel.: +82 62 970 2306; fax: +82 62 970 2304.
  E-mail addresses: samal@gist.ac.kr (S. Samal), jslee@gist.ac.kr (J.-S. Lee).

conjugated π-bridge. Most devices involved monolayers of such archetypal organic molecules sandwiched between two metal-electrodes, one bottom electrode plate and the tip of the atomic force microscope as the top contact electrode, or an ordered assembly of molecules in a nanopore or a nanogap connected to two electrodes [6]. Unimolecular rectification across a LB monolayer was first demonstrated for hexadecylquinolinium tricyanoquinodimethanide [5,6d,7], a D-π-A-type molecule.

Fullerenes are ideal materials for various nanoscale electronic devices. These molecules have a very strong affinity towards electrons. C_{60} is known as one of the strongest electron acceptors. When a suitable donor molecule is covalently or non-covalently bound to it, the donor–acceptor assembly shows many interesting properties with promising applications. For the rectification studies involving C_{60} derivatives, there should be an ordered assembly of preferably a monolayer of molecules over a suitable substrate. One of the deterrent factors, however, is that these molecules have a strong tendency to aggregate due to the hydrophobic fullerene–fullerene interactions [8]. This aggregation problem could easily be circumvented by attaching strong hydrophilic head groups to the fullerene [8f,9], blocking the contact of fullerene core by encapsulation [8g,10], and introducing structural constraints in the molecule [11]. Indeed, several amphiphilic fullerene derivatives are now known to form stable LB films at the air–water interface [12,13]. Similarly SAMs of fullerene derivatives, particularly those with appended thiol moiety, have produced highly ordered and densely packed structures on gold substrate [11]. The first C_{60}-based compound, dimethylaminophenylazafullerene [14], the LB film of which was sandwiched between two gold electrode layers, showed a tremendous apparent rectification ratio as high as 20,000, which was ascribed to the defects that grew at the domain boundaries. A Langmuir-Schaefer monolayer of another fullerene derivative [15] exhibited pronounced rectification with rectification ratio up to 16.5 when compared to the sample from the LB film. Interest in fullerene-based rectifier molecules with donor organic moiety
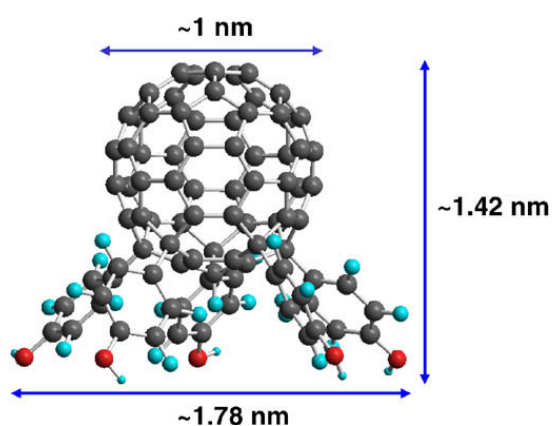
attached to the acceptor C_{60} through a suitable spacer continues unabated [16].

Herein, we report our studies on the monolayer of LB film of the fullerene pentapod formed at the air–water interface. The energy minimized structure of the molecule is shown in Fig. 1. This amphiphilic fullerene derivative is expected to form stable LB film at the air–water interface and afford a very robust structure through the five –OH groups anchored to the substrate. The electrical behavior of the film on Au(1 1 1) substrate measured using conducting atomic force microscopy (CAFM) showed that the molecule behaves as a rectifier when an appropriate bias voltage was applied. A suitable mechanism of rectification is proposed.

2. Experimental

2.1. Materials

The fullerene pentapod, $(4\text{-HOC}_6\text{H}_4)_5\text{HC}_{60}$, synthesized following the procedure reported by Nakamura and coworkers [17–19] was isolated in gram quantities in highly pure form. The compound is readily soluble in polar solvents like tetrahydrofuran, *N*-methyl pyrrolidinone, pyridine, and *N*,*N'*-dimethyl formamide. In nonpolar solvents like toluene solubility is low (∼0.001 g/ml). The compound is very stable towards oxidation under ambient conditions as studied by ^{1}H NMR monitoring the C–H peak intensity at 5.6 ppm. No change in spectral pattern was observed over a period of several weeks.

2.2. Computations

The geometry of free $(4\text{-HOC}_6\text{H}_4)_5\text{HC}_{60}$ was optimized using the density functional theory (DFT) method with the B3LYP functional [20] and the 6-31G** basis set. The HOMO and LUMO energy levels were determined on the final geometry by reading the DFT eigenvalues as well as by calculating the ionization potential ($IP = E_{\text{CATION}} - E_{\text{NEUTRAL MOLECULE}} \approx -E_{\text{HOMO}}$) and electron affinity ($EA = E_{\text{NEUTRAL MOLECULE}} - E_{\text{ANION}} \approx -E_{\text{LUMO}}$). In order to estimate roughly the error attributable to the functional-dependence of DFT, the energy levels were estimated using both B3LYP (hybrid) and PBE (GGA) functionals [21]. It should be noted that though the device in the present case is metal-organic-metal type, the shift and broadening of the energy levels due to the substrate (Au) were not taken into account in our calculations on this "free" isolated molecule. All the calculations were done with Jaguar v6.5 (Schrodinger Inc., Portland, OR).

2.3. Langmuir-Blodgett film

The LB film was cast using a PC controlled KSV MINITROUGH instrument attached to a constant temperature bath. The quality of the LB monolayer at the air–water interface was monitored by KSV Win LB computational program. A 70 µl dilute solution of the fullerene pentapod (0.0235 mg/ml in toluene) was spread on the air–water interface and the trough area decreased at a rate of 200 cm^2/min. The film was transferred at a constant rate

Fig. 1. Energy minimized structure of 1,4,11,15,30-pentakis(4-hydroxyphenyl)-2H-1,2,4,11,15,30-hexahydro-[60]fullerene, $(4\text{-HOC}_6\text{H}_4)_5\text{HC}_{60}$, the amphiphilic fullerene pentapod, with molecular dimensions. Color code: grey – carbon, green – hydrogen, and red – oxygen. (For interpretation of the references to color in this figure legend, the reader is referred to the web version of this article.)

of 5 mm/min and a surface pressure of 20 mN/M onto a freshly prepared hydrophilic Au(1 1 1) substrate, which was submerged in the subphase before spreading and compressing the LB film. All the experiments were performed at 21 °C using pure deionized water as the subphase.

2.4. Atomic force microscopy

The LB film was examined by atomic force microscopy (AFM) to determine the height of the particles. The AFM images were acquired with a Nanoscope III dimension (Digital Instruments Inc. Santa Barbara, CA). Super sharp silicon taping mode with a cantilever (Nanosensor, Wetzlar-Blankenfeld, Germany) having resonance frequency of ca. 330 kHz and scan rate of 0.5 Hz was used. The tip of the cantilever has a normal radius of ca. 2 nm. The samples for AFM measurement were prepared by LB deposition method at the air–water interface over Au(1 1 1) substrate.

2.5. Ellipsometry

Variable angle spectroscopic ellipsometry measurement was done on a NFT I-ELLI 2000 ellipsometer equipped with a Nd:YAG LASER at 65º, 70º and 75º angles of incidence in the wavelength range of 300–1000 nm. The optical constants for bare gold were measured immediately before measuring the fullerene pentapod film-coated substrate. A refractive index of 1.533 was assumed for all measurements. The thickness of the film using three samples was calculated from variation of the ellipsometric parameters Δ and Ψ. Repeated measurements were made at different positions all through the substrate for obtaining accurate results.

2.6. Contact angle measurement

The wettability of the LB film was investigated by measuring the contact angle of water of a freshly prepared sample using CA-S150, KYOWA instrument. Ten microlitre of ultra pure water (Barnstead Easypure LF, 18.3 MΩ cm) was used throughout the experiment. The contact angle was read only on one side of the drop.

2.7. Conducting atomic force microscopy

Samples for CAFM measurements are the fullerene pentapod LB films transferred over Au(1 1 1) substrate. These were dried in a vacuum desiccator for 48 h prior to the electrical measurements. Precautions were taken to prevent damage to the film in view of its fragile nature by thermal radiation. Current–voltage (I–V) measurement was performed using a commercially available AFM system (PSIA, XE-100 model) with conductive AFM tips that were made from Au (20 nm)/Cr (20 nm) coating around conventional AFM tips. Two terminal DC I–V data were acquired using a semiconductor parameter analyzer (HP4145B). Voltage was applied to CAFM tip while the Au substrate was grounded. All the electrical measurements were carried out inside a covered AFM chamber through which nitrogen gas was passed to minimize the formation of contaminants on the surface of the film. From Johnson–Kendall–Roberts (JKR) model [22] the radius of the contact area under the CAFM tip was estimated to be less than 10 nm [23].

3. Results and discussion

3.1. Computations

The outer diameter of C_{60} is ~1 nm estimated by taking into account the size of the π-electron cloud associated with the carbon atoms [24]. This value was taken as the diameter of the fullerene moiety in the pentapod (see Fig. 1). The five phenolic groups form a circular face, the diameter of which was ~1.78 nm. The difference between the diameters of the top fullerene moiety and bottom circular face is 0.78 nm. This is large enough to prevent fullerene–fullerene interaction among the neighboring molecules if uniformly oriented in a monolayer. Similar observations have been made for fullerene derivative C_{60}-MPPA [11] where aggregation was prevented due to the difference in size between the fullerene head group attached to a relatively larger MPAA unit.

In the study of molecular electronics, computational calculations of the molecular energy levels relative to metal-electrode energies bear specific significance. Such calculations have been made for several fullerene derivatives [14,15,25]. Even though the device in the present case is metal-organic-metal type, the shift and broadening of these energy levels due to the substrate (Au) was not taken into account in our calculations on the "free" isolated molecule. Thus, the calculated HOMO and LUMO levels, shown in Fig. 2, should be taken as approximate.

The two functionals of DFT, B3LYP and PBE, result in essentially the same electronic structure. Both of them predict the same molecular energy diagram. The HOMO and HOMO − 1 are very close in energy and hence considered as degenerate MOs, and similarly the LUMO and LUMO + 1 constitute a pair of degenerate orbitals. The energy levels taken from the B3LYP eigenvalues are as follows (in eV): −5.45 (E_{HOMO}), −5.47 ($E_{HOMO − 1}$), −5.63 ($E_{HOMO − 2}$), −5.84 ($E_{HOMO − 3}$), −5.94 ($E_{HOMO − 4}$), and −5.96 ($E_{HOMO − 5}$) for the HOMO levels; −2.47 (E_{LUMO}), −2.45 ($E_{LUMO + 1}$), and −2.32 ($E_{LUMO + 2}$) for the LUMO levels. Both functionals also predict that the frontier MOs of the molecule are essentially localized on the same C_{60} moiety, which is in sharp contrast to other fullerene derivative-based donor–acceptor systems studied for molecular rectification where the donor HOMO is located on the exocyclic group and the acceptor LUMO is on C_{60} [14–16,26].

The two functionals, however, show discrepancy in the precise locations of these energy levels (Table 1). The HOMO–LUMO gaps calculated with B3LYP are significantly larger than those calculated with PBE, as observed previously [27]. Interestingly this discrepancy becomes small when estimated from the IP and EA values. Since the PBE functional is known to underestimate the HOMO–LUMO gap, we focus on analyzing the experimental data only based on the two B3LYP values in the following discussion.
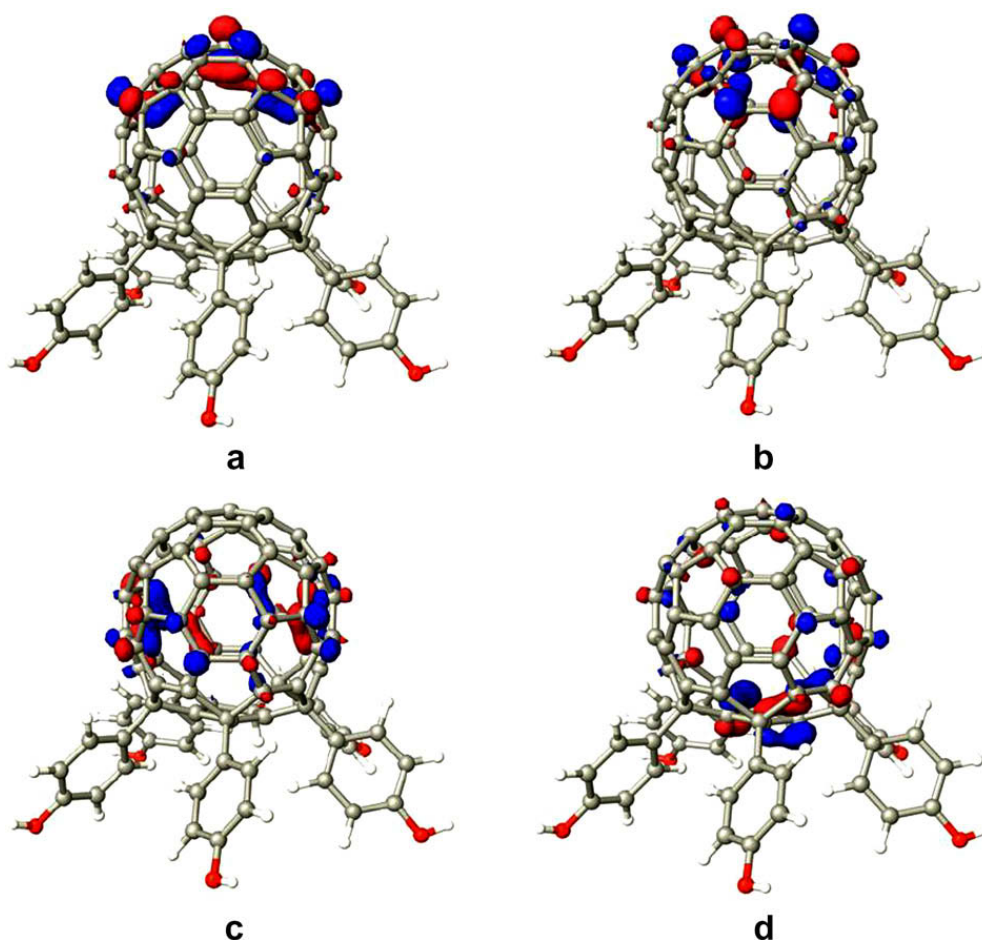
Fig. 2. Molecular orbitals of the fullerene pentapod generated by DFT calculations (B3LYP/6-31G**). (a) LUMO (-2.47 eV) (b) LUMO + 1 (-2.45 eV), (c) HOMO (-5.45 eV), and (d) HOMO $-$ 1 (-5.47 eV). Color code: grey – carbon, white – hydrogen, and red – oxygen. (For interpretation of the references to colour in this figure legend, the reader is referred to the web version of this article.)

Table 1
HOMO–LUMO gap calculated by B3LYP and PBE functionals.

Method	E_{HOMO} (eV)	E_{LUMO} (eV)	HOMO–LUMO gap (eV)
B3LYP	-5.5	-2.5	3.0
B3LYP IP/EA	-6.3	-1.6	4.7
PBE	-4.8	-3.0	1.8
PBE IP/EA	-5.9	-1.7	4.2

3.2. LB film

The LB pressure-area isotherm of the fullerene pentapod is shown in Fig. 3. From the isotherm, the mean molecular area per molecule, A_0, obtained by extrapolating the pressure-area isotherm to zero pressure was 0.98 nm^2 molecule^{-1}, which corresponds to a mean diameter of 1.117 nm per molecule. The LB films of unmodified dilute C$_{60}$ solution show a limiting area of 0.98 nm^2 molecule^{-1} [8a,8c,8e], as against the theoretically predicted value of 0.866 nm^2 molecule^{-1} for a monolayer of the molecule [9b,28]. This suggested that the pentapod formed a monolayer at the air–water interface rather than an irreversible aggregation of the fullerene clusters [12]. The mean molecular area at the inflection point (A_c) calculated at the collapse pressure Π_c of 33 mN/M was 0.83 nm^2 molecule^{-1}. Above the collapse pressure, the nature of the
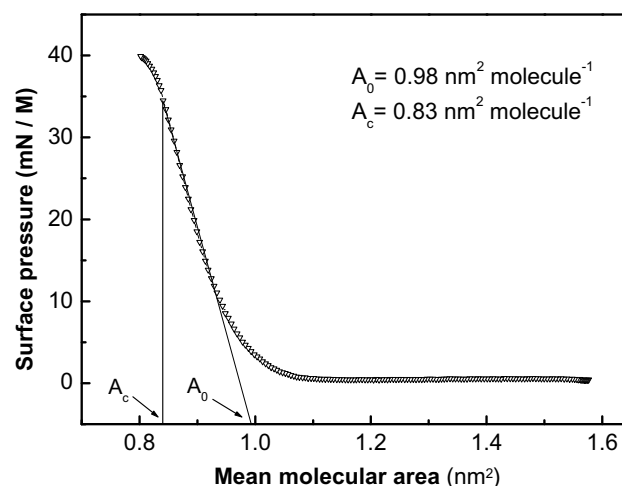
Fig. 3. Pressure–area isotherm (Π-A) of the LB film at the air–water interface obtained by spreading the fullerene pentapod solution in toluene.

curve changed indicating phase transition, possibly from one closely packed structure to another. The pentapod was transferred atop the Au(111) substrate at a transfer pressure, Π_{tr}, of 20 mN/M. The mean molecular area at the transfer pressure, A_{tr}, was 0.90 nm^2 molecule^{-1}, from

which the mean diameter per molecule was calculated to be ~1.07 nm.

The diameter of the bottom circular face of the molecule calculated from computational measurement is ~1.78 nm. This should be the nearest neighbor distance between the molecules if they are in direct contact. However, an examination of the energy minimized structure of the molecule showed that there is enough space between the phenolic rings to allow the neighboring molecules to interdigitate as schematically shown in Fig. 4. This evidently means that the molecules could be packed more closely than 1.78 nm, i.e., even when the mean molecular diameter was 1.07 nm, the molecules could still form a monolayer without vertical stacking. It may be noted here that the molecules in the LB film though seem to interdigitate at the transfer pressure could get organized further while drying to optimize the intermolecular order. The mean molecular area of 1.07 nm is in close agreement with the nearest neighbor distance in a close-packed (1 1 1) plane of the C_{60} molecules [8e]. The LB film of C_{60}, $C_{60}O$ and $C_{61}H_2$ showed (1 1 1) close-pack arrangement for the molecules with nearest neighbor distances of 1.002, 1.003 and 1.003 nm, respectively. Hexagonal (1 1 1) face-centered cubic lattice with neighboring distance of 0.95 nm is reported for other fullerene derivatives [29].

The thickness of the LB film, determined from ellipsometry (1.5 ± 0.01 nm) and the height image of atomic force microscopy (AFM) studies (Fig. 5), was consistent with the height of the molecule from computational measurement. Thus, the LB film is mostly a monolayer of the molecules. Water contact angle of the film on Au(1 1 1) substrate was 97°. The high contact angles of H_2O on LB film suggested the hydrophobic nature of the film, which is expected of the film with the fullerene moieties exposed to air. Thus the molecule on the substrate surface formed a homogeneous monomolecular film with the five functional groups anchored to the substrate leading to a robust structure without aggregation. Recently Nakamura and coworkers [30] have reported the photophysical properties of the monolayer of the benzoic acid derivative of a series of fullerene penta-addition derivatives, which show the same anchoring behavior to the substrate.

Control experiments were performed using two other fullerene penta-addition derivatives, $(C_6H_5)_5HC_{60}$ and $(4-CH_3SC_6H_4)_5HC_{60}$. From the pressure-area isotherms, A_0 was 1.98 nm^2 $molecule^{-1}$ for $(C_6H_5)_5HC_{60}$ and
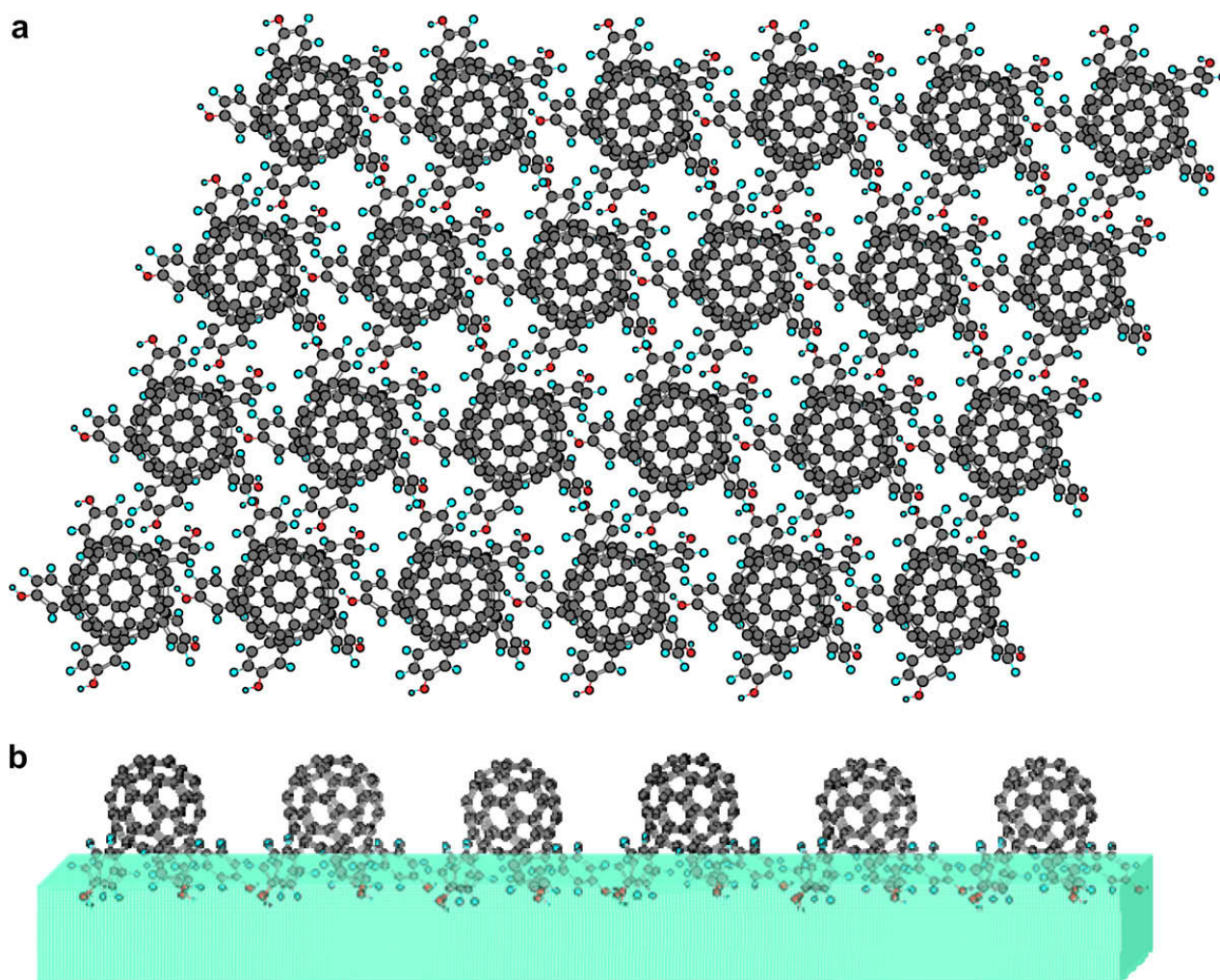
Fig. 4. Schematic arrangement of fullerene pentapods in the LB film. (a) Top view of the molecules showing the phenolic groups of neighboring molecules to interdigitate resulting in close-packing of the molecules. (b) Side view of the molecules showing arrangement at the air–water interface (shown for a single row of molecules).
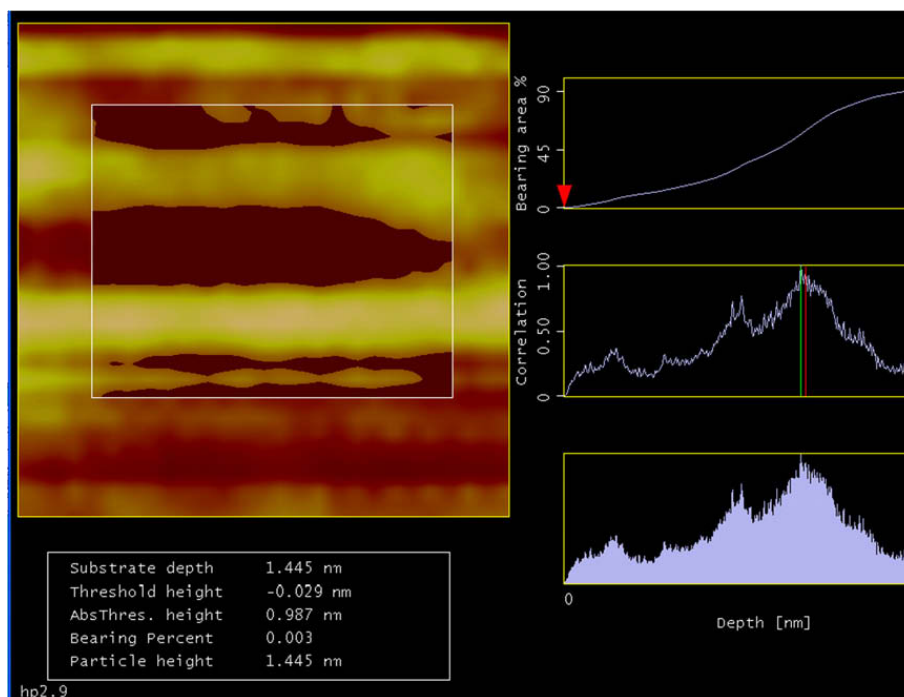
Fig. 5. Atomic force microscopy picture of the (4-HOC$_6$H$_4$)$_5$HC$_{60}$ LB film on Au(1 1 1) substrate showing particle height of 1.445 nm.

2.09 nm^2 molecule^{-1} for (4-CH$_3$SC$_6$H$_4$)$_5$HC$_{60}$, which correspond to mean diameters of 1.587 nm and 1.631 nm per molecule, respectively. In comparison, the mean diameter of (4-HOC$_6$H$_4$)$_5$HC$_{60}$ was 1.117 nm per molecule. The large molecular diameters of (C$_6$H$_5$)$_5$HC$_{60}$ and (4-CH$_3$SC$_6$H$_4$)$_5$HC$_{60}$ imply that the derivatives are randomly oriented at the air–water interface due to their poor amphiphilic nature.

3.3. I–V measurement

The *I–V* measurements for the LB films of the fullerene pentapods performed using CAFM method [31] with gold as the top and the bottom electrodes is schematically shown in Fig. 6. The LB monolayer exhibited electrical rectification when a positive bias was applied to the CAFM tip (Fig. 7). The *I–V* characteristics showed current rectification at bias voltage of ±1.0 V measured at different monolayer junctions, with high rectification ratios (RR) registered at each junction. The LB monolayer exhibited larger current flow when a positive bias was applied to the CAFM tip. In this condition, current flows from the CAFM tip top electrode to the bottom gold electrode. The direction of electron transport as shown in Fig. 6 is opposite to that seen in previous unimolecular rectifiers using either Al or Au electrodes [6b,6d,6g,7c,14]. Our observation on the direction of rectification is consistent with elastic transport model [32] and opposite to that predicted by Aviram–Ratner inelastic transport model [3].

Fig. 8 represents the *I–V* curves of the pentapod LB film measured up to higher bias voltages of ±1.5 V, ±2.0 V, ±2.5 V, and ±3.0 V. In the bias voltages ±1.0 V, ±1.5 V, and ±2.0 V high current asymmetries were observed with rectification ratios of 1.3–48.0, 2.0–32.6, and 2.0–19.5, respectively. However, further increase of voltage sweep up to
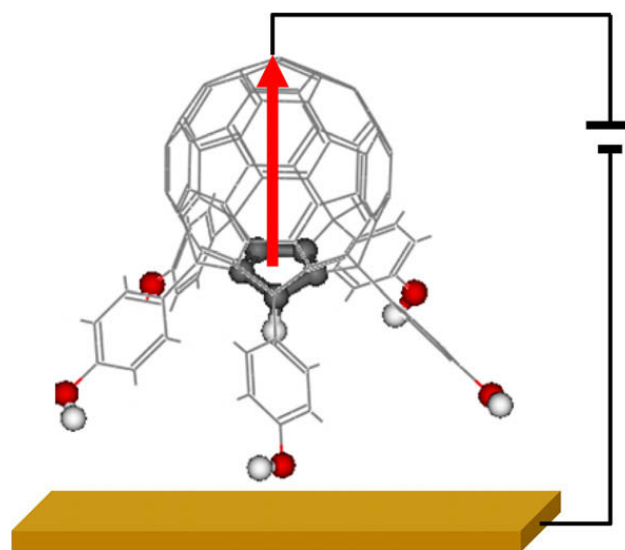
Fig. 6. Schematic representation of the *I–V* measurement of the fullerene pentapod by CAFM. The arrow indicates the direction of electron transport when positive bias is applied to the CAFM tip (top electrode). The Au substrate (bottom electrode) is grounded.

±2.5 V led to gradual increase in current in the negative bias direction with lowering of rectification ratios to 1.0 at ±2.5 V and 0.9 at ±3.0 V. Thus current asymmetricity was substantially reduced for higher voltage sweeps. The best results were obtained at bias voltages of ±1.0 V and ±1.5 V, when there was negligible current flow in the negative bias direction. Current started flowing in the negative direction once the bias voltage exceeded ±1.5 V. The asymmetric nature persisted with gradual lowering of RR and at ±2.5 V the *I–V* curve became symmetrical (RR ≈ 1). A plausible explanation for such behavior is presented (see below).
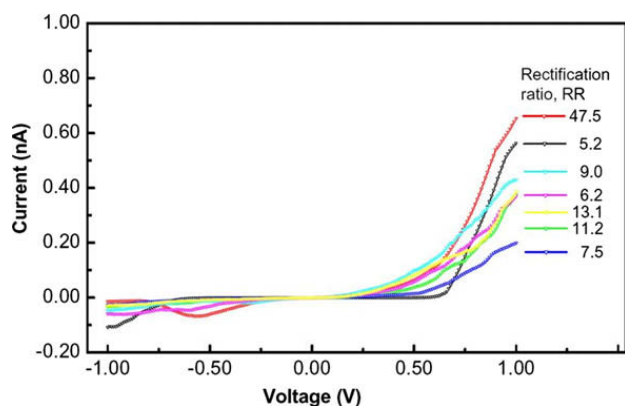
Fig. 7. *I–V* characteristics of the LB film of the fullerene pentapod showing current rectification at bias voltage of ±1.0 V measured at different junction positions, with high rectification ratios (RR) registered at each junction.

The *I–V* measurements were taken repeatedly by changing the position of the CAFM tip and the rectification ratio for each position was recorded. It was observed that the molecule showed rectification behavior in almost 80% of the devices measured. From the statistical histograms (Fig. 9) the mean rectification ratios were 10.8 and 14.7, at bias voltages of ±1.0 V and ±1.5 V, respectively.

The *I–V* characteristics of LB films from fullerene penta-derivatives, $(C_6H_5)_5HC_{60}$ and $(4-CH_3SC_6H_4)_5HC_{60}$ were studied. For these molecules no rectification was observed in the same applied tip bias voltage ranges in which the fullerene pentapod $(4-HOC_6H_4)_5HC_{60}$ showed rectification. Evidently, in the LB films, $(C_6H_5)_5HC_{60}$ and $(4-CH_3SC_6H_4)_5HC_{60}$ are not as uniformly oriented as the highly amphiphilic $(4-HOC_6H_4)_5HC_{60}$. Furthermore, the *I–V* characteristics of the alkane thiol SAMs under a similar experimental set up used for the present study were symmetric with a mean RR value of 1.17 [33a]. Thus, the observed current rectification behavior of $(4-HOC_6H_4)_5HC_{60}$ is a characteristic attributable to the typical structural feature of the pentapod.

3.4. Mechanism of electron transport

The mechanism of the electron transport is explained by the interaction between the molecular energy levels obtained from the DFT calculation of the fullerene pentapod and the Fermi level of the electrode. Here the work function of Au was taken as −4.6 eV though in the literature there is considerable variation of this value from −4.70 eV to −5.40 eV [34], depending upon the crystal face of Au and the method of measurement.

According to the B3LYP eigenvalues the HOMO and LUMO energies of the free molecule are separated by 2.98 eV, but this separation is expected to be smaller in the actual device as the interaction with the electrodes would broaden the molecular energy levels. At zero bias, the HOMO and HOMO − 1 levels of the free molecule are located ∼0.9 eV below the Fermi level (E_F) of Au, and the LUMO and LUMO + 1 levels are located ∼2.1 eV above the E_F.

When a bias of +1.0 V is applied to the top electrode, E_F of Au goes down approximately by 1 eV relative to the cathode and becomes −5.6 eV, approaching resonance with the HOMO and HOMO − 1 levels of the molecule (E_{HOMO} = −5.45 eV, $E_{HOMO − 1}$ = −5.47 eV) (Fig. 10). Hence current flow in the forward direction is favored. When a negative bias voltage (−1.0 V) is applied to the top electrode, the E_F of Au goes up to −3.6 eV, and neither the HOMOs nor the LUMOs are aligned with the electrode energy levels, thus impeding current flow in the reverse
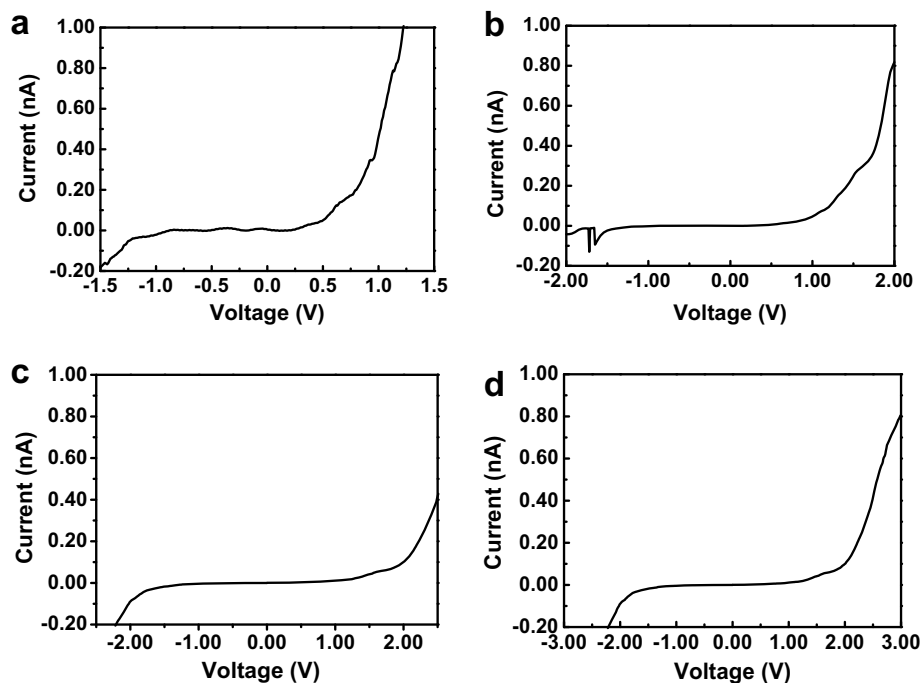
Fig. 8. Typical *I–V* plots measured up to a higher bias than ±1.0 V. (a) RR = 12.0 at ±1.5 V, (b) RR = 19.5 at ±2.0 V, (c) RR = 1.0 at ±2.5 V, and (d) RR = 0.9 at ±3.0 V.
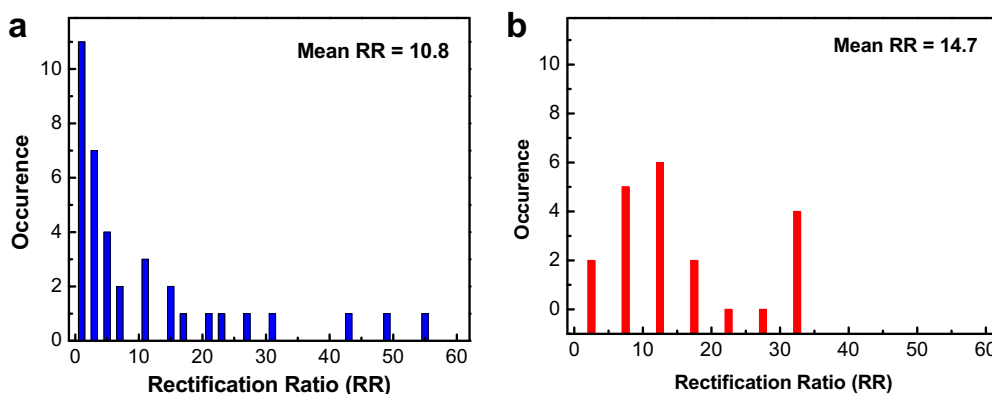
Fig. 9. Statistical histograms of rectification ratio data showing mean RR values of (a) 10.8 at ±1.0 V and (b) 14.7 at ±1.5 V.
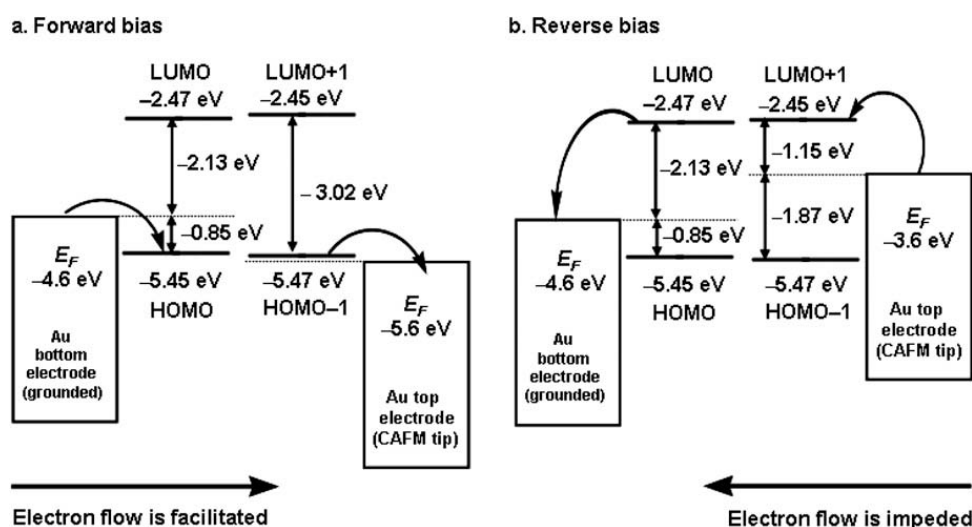
Fig. 10. Energy levels of the device under applied bias voltage. (a) A forward bias voltage of +1.0 V facilitates the electron transport from the bottom Au electrode to the top CAFM tip electrode, and (b) a reverse bias voltage of −1.0 V impedes it in the opposite direction. The HOMO and HOMO − 1 levels are of nearly similar energy and so are LUMO and LUMO + 1. Hence these are shown to take part in the electron tunneling process as though they are degenerate orbitals.

direction. When a bias voltage of +2.0 V is applied (E_F = −6.6 V), lower HOMO levels, such as HOMO − 10 ($E_{HOMO − 10}$ = −6.22 eV), become energetically favorable and participate in the current flow process. At −2.0 V the LUMO levels (E_{LUMO} = −2.47 eV, $E_{LUMO + 1}$ = −2.45 eV) approach resonance with E_F of Au (−2.6 V). Hence, some current starts flowing in the reverse direction as well. Apparently, for higher bias voltages, lower HOMO − X and upper LUMO + X levels had energies aligned to a similar extent with E_F of Au, facilitating current flow in both the directions with equal ease.

It may be pointed out here that the conventional use of the one-electron molecular orbitals from a DFT calculation may be an approximation to the many-electron states that will influence the real transport processes. Nevertheless, it is not actually the reaching of resonances that leads to the rectification but rather the approaching of resonances. Hence the explanation of charge transport in a preferred direction based on alignment of calculated orbital energies with those of the Fermi levels of the electrodes using the present method of computation, though qualitative, is a rational approach at the moment.

Besides, in the present case, there is homo-conjugation [35] between the cyclopentadiene moiety with the rest of the 50 sp^2 carbon atoms of the fullerene and peri-conjugation [36] between the p_z-π orbitals of phenolic groups and orbitals of adjoining fullerene carbon atoms. Thus, the phenolic groups, the cyclopentadiene moiety, and the rest of the fullerene molecule in the pentapod electronically interact. From the B3LYP calculation it was found that the fullerene pentapod has a high ground state dipole moment of 3.23 debye (4.53 debye calculated from PBE), and hence the molecule is quite polar. C_{60} accepts six electrons electrochemically to form hexa-anion whereas oxidation is relatively difficult [37]. The electron affinity of C_{60} is 2.65 ± 0.05 eV and the first ionization potential is 7.58 eV [38]. The values for the hydroxypentapod, calculated using B3LYP/6-31G**, are 1.6 eV and 6.3 eV, respectively (1.7 eV and 5.9 eV from PBE/6-31G**). Thus, the pentapod has retained to a significant extent the characteristic electron-withdrawing ability of C_{60}. Considering that the C_{50} moiety of the pentapod is still strongly electron-withdrawing, the direction of the dipole moment must be towards the fullerene moiety. Besides, the molecule could undergo further

polarization in this direction when a positive bias is applied to the CAFM tip electrode. Hence electron transport in the forward bias condition should be facilitated, as has been actually observed. Similar rectification behavior has been explained by polarization of the electron cloud of the molecule under an applied potential [39].

Three mechanisms, S-, A- or U-types, have been suggested to explain current rectification in metal-organic-metal devices [5,7a]. When the current passing through a molecule involves electron transfer between its own molecular orbitals, or asymmetry in the molecule itself causes asymmetry in current flow it is called the U-type of electrical rectification. Previously, the mechanism of electrical rectification in fullerene derivatives involve electron transfer in which C_{60} acts as an acceptor and exohedral functional groups attached to it act as donors [14,16,26]. The donor is attached to the acceptor by a σ-bond and there is through-bond electron transfer from the HOMO of the donor to the LUMO of the acceptor. However, in the present case, both the HOMO and the LUMO are in the same fullerene cage interacting with each other through homo-conjugation. Under a suitable applied bias, electron from the HOMO level is transferred to the LUMO level through the fullerene cage itself. This is completely a new case observation in the field of molecular rectification of the fullerene derivatives and a novel example of a true U-type unimolecular rectifier.

4. Conclusions

An amphiphilic fullerene pentapod, $(4\text{-}HOC_6H_4)_5HC_{60}$, formed well-defined LB film at the air–water interface and constitutes mostly a monomolecular arrangement with C_{60} facing upwards. The LB film transferred over Au(1 1 1) substrate afforded a robust structure through anchoring of the five phenolic –OH groups. When the device was subjected to a forward bias using the CAFM tip as the top electrode in contact with the fullerene moiety, electrons moved from the bottom negative electrode to the top electrode through the fullerene molecule. When a negative bias was applied to the CAFM tip electron transport was significantly less in the opposite direction. The rectification was appreciable up to an applied bias of ±2.0 V; decreasing thereafter until at ±2.5 V there was no rectification. Two other fullerene derivatives, $(C_6H_5)_5HC_{60}$ and $(4\text{-}CH_3SC_6H_4)_5HC_{60}$, did not show any electrical rectification. These molecules are not as uniformly oriented on the substrate surface in contrast to $(4\text{-}HOC_6H_4)_5HC_{60}$. Thus, $(4\text{-}HOC_6H_4)_5HC_{60}$ constitutes a new class of molecule, in which the donor HOMO and acceptor LUMO levels are on the same fullerene cage and hence represent true unimolecular U-type rectifier.

Acknowledgements

References

[1] C. Joachim, J.K. Gimzewski, A. Aviram, Nature 408 (2000) 541.
[2] (a) F.L. Carter (Ed.), Molecular Electronic Designs I, Marcel Dekker, New York, 1987;
(b) F.L. Carter (Ed.), Molecular Electronic Designs II, Marcel Dekker, New York, 1987.
[3] A. Aviram, M. Ratner, Chem. Phys. Lett. 29 (1974) 277.
[4] (a) G.J. Ashwell, J.R. Sambels, A.S. Martin, W.G. Parker, M. Szablewski, J. Chem. Soc., Chem. Commun. (1990) 1374;
(b) A. Martin, J.R. Sambles, G.J. Ashwell, Phys. Rev. Lett. 70 (1993) 218;
(c) G.J. Ashwell, R. Hamilton, L.R.H. High, J. Mater. Chem. 13 (2003) 1501. The current rectification ratio is 11 at 1 V (The limiting currents on the vertical axis of Figure 2 of the communication should read from +1.0 nA to −1.0 nA rather than from +10 nA to −10 nA);
(d) G.J. Ashwell, W.D. Tyrell, A.J. Whittam, J. Mater. Chem. 13 (2003) 2855. SAMs of a D-σ-A dye linked via S-C_3H_6 to a gold coated substrate alters its *I–V* characteristics from asymmetric to symmetric when the intramolecular charge-transfer is disrupted by protonation.
[5] (a) R.M. Metzger, Acc. Chem. Res. 32 (1999) 950;
(b) R.M. Metzger, Chem. Rev. 103 (2003) 3803.
[6] (a) A.C. Brady, B. Hodder, A.S. Martin, J.R. Sambles, C.P. Ewels, R. Jones, P.R. Briddon, A.M. Musa, C.A. Panetta, D.L. Mattern, J. Mater. Chem. 9 (1999) 2271;
(b) J.W. Baldwin, R.R. Amaresh, I.R. Peterson, W.J. Shumate, M.P. Cava, M.A. Amiri, R. Hamilton, G.J. Ashwell, R.M. Metzger, J. Phys. Chem. B 106 (2002) 12158;
(c) J. Ferraris, D.O. Cowan, V. Walatka Jr., J.H. Perlstein, J. Am. Chem. Soc. 95 (1973) 948;
(d) R.M. Metzger, T. Xu, I.R. Peterson, J. Phys. Chem. B 105 (2001) 7280;
(e) G.J. Ashwell, A. Chwialkowska, L.R.H. High, J. Mater. Chem. 14 (2004) 2389;
(f) D. Vuillaume, B. Chen, R.M. Metzger, Langmuir 15 (1999) 4011;
(g) T. Xu, I.R. Peterson, M.V. Laxmikantham, R.M. Metzger, Angew. Chem. Int. Ed. 40 (2001) 1749;
(h) G.J. Ashwell, W.D. Tyrell, A.J. Whittam, J. Am. Chem. Soc. 126 (2004) 7102.
[7] (a) R.M. Metzger, Chem. Record 4 (2004) 291;
(b) B. Chen, R.M. Metzger, J. Phys. Chem. B 103 (1999) 4447;
(c) R.M. Metzger, B. Chen, U. Hopfner, M.V. Lakshmikantham, D. Vuillaume, T. Kawai, X. Wu, H. Tachibana, T.V. Hughes, H. Sakurai, J.W. Baldwin, C. Hosch, M.P. Cava, L. Brehmer, G.J. Ashwell, J. Am. Chem. Soc. 119 (1997) 10455.
[8] (a) Y. Obeng, A. Bard, J. Am. Chem. Soc. 113 (1991) 6279;
(b) T. Nakamura, H. Tachibana, M. Yumura, M. Matsumoto, R. Azumi, M. Tanaka, Y. Kawabata, Langmuir 8 (1992) 4;
(c) C. Jehoulet, Y. Obeng, Y. Kim, F. Zhou, A. Bard, J. Am. Chem. Soc. 114 (1992) 4237;
(d) L. Bulhoes, Y. Obeng, A. Bard, Chem. Mater. 5 (1993) 110;
(e) N.C. Maliszewskyj, P.A. Heiney, D.R. Jones, R.M. Strongin, M.A. Cichy, A.B. Smith III, Langmuir 9 (1993) 1439;
(f) J. Gallani, D. Felder, D. Guillon, B. Heinrich, J. Nierengarten, Langmuir 18 (2002) 2908;
(g) P. Wang, M. Shamsuzzoha, X. Wu, W. Lee, R.M. Metzger, J. Phys. Chem. 96 (1992) 9025.
[9] (a) C. Hawker, P. Saville, J. White, J. Org. Chem. 59 (1994) 3503;
(b) M. Maggini, A. Karlsson, L. Pasimeni, G. Scorrano, L. Valli, Tetrahedron Lett. 35 (1994) 2985;
(c) M. Maggini, L. Pasimeni, M. Prato, G. Scorrano, L. Valli, Langmuir 10 (1994) 4164;
(d) S. Ravaine, F. Lepecq, C. Mingotaud, P. Delhaes, J. Hummelen, F. Wudl, L. Patterson, J. Phys. Chem. 99 (1995) 9551;
(e) M. Carrano, P. Ceroni, F. Paolucci, S. Roffia, T. Da Ros, M. Prato, M. Sluch, C. Pearson, M. Petty, M. Bryce, J. Mater. Chem. 10 (2000) 269;
(f) D. Guldi, M. Maggini, S. Mondini, F. Guerin, J. Fendler, Langmuir 16 (2000) 1311;
(g) J. Jin, L. Li, Y. Li, Y. Zhang, X. Chen, D. Wang, S. Jiang, T. Li, L. Gan, C. Huang, Langmuir 15 (1999) 4565.
[10] (a) P. Wang, R.M. Metzger, B. Chen, Thin Solid Films 329 (1998) 96;
(b) J. Nierengarten, C. Schall, J. Nicoud, B. Heinrich, D. Guillon, Tetrahedron Lett. 39 (1998) 5747;
(c) G. Felder, J. Gallani, D. Guillon, B. Heinrich, J. Nicoud, J. Nierengarten, Angew. Chem. Int. Ed. 39 (2000) 201;
(d) J. Nierengarten, Chem. Eur. J. 6 (2000) 3667;

(e) D. Felder, M. Carreon, J. Gallani, D. Guillon, J. Nierengarten, C. Thierry, R. Deschenaux, Helv. Chim. Acta 84 (2001) 1119.

[11] S.H. Kang, H. Ma, M.-S. Kang, K.S. Kim, A. K.-Y. Jen, M.H. Zareie, M. Sarikaya, Angew. Chem. Int. Ed. 43 (2004) 1512.

[12] Y. Gao, Z. Tang, E. Watkin, J. Majweski, H.L. Wang, Langmuir 21 (2005) 1416.

[13] T. Kawai, S. Scheib, P.M. Cava, R.M. Metzger, Langmuir 13 (1997) 5627.

[14] R.M. Metzger, J.W. Baldwin, W.J. Shumate, I.R. Peterson, P. Mani, G.J. Mankey, T. Morris, G. Szulczewski, S. Bosi, M. Prato, A. Comito, Y. Rubin, J. Phys. Chem. B 107 (2003) 1021.

[15] A. Honcius, A. Jaiswal, A. Gong, K. Ashworth, C.W. Spangler, I.R. Peterson, L.R. Dalton, R.M. Metzger, J. Phys. Chem. B 109 (2005) 857.

[16] A. Honcius, R.M. Metzger, A. Gong, C.W. Spangler, J. Am. Chem. Soc. 129 (2007) 8310.

[17] M. Sawamura, K. Kawal, Y. Matsuo, K. Kanie, T. Kato, E. Nakamura, Nature 419 (2002) 702.

[18] (a) M. Sawamura, H. Likura, E. Nakamura, J. Am. Chem. Soc. 118 (1996) 12850;
(b) M. Sawamura, H. Likura, H. Ohama, U.E. Hackler, E. Nakamura, J. Organometal. Chem. 599 (2000) 32;
(c) M. Sawamura, M. Toganoh, Y. Kuninobu, S. Kato, E. Nakamura, Chem. Lett. (2000) 262;
(d) M. Sawamura, N. Nagahama, M. Toganoh, E. Nakamura, J. Organometal. Chem. 652 (2002) 31.

[19] E. Nakamura, M. Sawamura, Pure Appl. Chem. 73 (2) (2001) 355.

[20] (a) J.C. Slater, Quantum Theory of Molecules and Solids. The Self-Consistent Field for Molecules and Solids, vol. 4, McGraw Hill, New York, 1974;
(b) A.D. Beck, Phys. Rev. A 38 (1998) 3098;
(c) S.H. Vosko, L. Will, M. Nusair, Can. J. Phys. Chem. 58 (1980) 1200;
(d) C. Lee, W. Yang, R.G. Parr, Phys. Rev. B 37 (1998) 785;
(e) B. Miehlich, A. Savin, H. Stoll, H. Preuss, Chem. Phys. Lett. 157 (1988) 200.

[21] (a) J.P. Perdew, K. Burke, M. Ernzerhof, Phys. Rev. Lett. 77 (1996) 3865;
(b) J.P. Perdew, K. Burke, M. Ernzerhof, Phys. Rev. Lett. 78 (1997) 1396.

[22] K.L. Johnson, K. Kendall, A.D. Robert, Proc. Roy. Soc. Lond. A 324 (1971) 301.

[23] T. Lee, W. Wang, J.F. Klemic, J.J. Zhang, J. Su, M.A. Reed, J. Phys. Chem. B 108 (2004) 8742.

[24] (a) R. Tycko, R.C. Haddon, G. Dabbagh, S.H. Glarum, D.C. Douglass, A.M. Mujsce, J. Phys. Chem. 95 (1991) 518;
(b) R.D. Johnson, D.S. Bethume, C.S. Yannoni, Acc. Chem. Res. 25 (1992) 169.

[25] A. Hirsh, I. Lamparth, T. Grösser, J. Am. Chem. Soc. 116 (1994) 9385.

[26] S.S. Gayatri, A. Patnaik, Chem. Commun. (2006) 1977.

[27] (a) Y.H. Jang, W.A. Goddard III, J. Phys. Chem. C 112 (2008) 8715;
(b) Y.H. Jang, S. Hwang, Y.H. Kim, S.S. Jang, W.A. Goddard III, J. Am. Chem. Soc. 126 (2004) 12636.

[28] P.A. Heiney, J.E. Fischer, A.R. McGhie, W.J. Romanow, A.M. Denenstein, J.P. McCauley Jr., A.B. Smith III, D.-E. Cox, Phys. Rev. Lett. 66 (1991) 2911.

[29] M. Matsumoto, H. Tachibana, R. Azumi, M. Tanaka, J. Nakamura, Langmuir 11 (1995) 660.

[30] Y. Matsuo, K. Kanaizuka, K. Matsuo, Y.-W. Zhong, T. Nakae, E. Nakamura, J. Am. Chem. Soc. 130 (2008) 5016.

[31] (a) L. Andolfi, S. Cannistraro, Surface Science 598 (2005) 68;
(b) D.J. Wold, C.D. Frisbie, J. Am. Chem. Soc. 123 (2001) 5549;
(c) J. Zhao, K. Uosaki, Nanoletter 2 (2002) 137;
(d) X.D. Cui, A. Primak, X. Zarate, J. Tomfohr, O.F. Sankey, A.L. Moore, T.L. Moore, D. Gust, G. Harris, S.M. Lindsay, Science 294 (2001) 571;
(e) J.M. Beebe, V.B. Engelkes, L.L. Miller, C.D. Frisbe, J. Am. Chem. Soc. 124 (2002) 11268;
(f) X.D. Cui, A. Primak, X. Zoarate, J. Tomfohr, O.F. Sankey, A.L. Moore, T.A. Moore, D. Gust, G. Harris, S.M. Lindsay, Nanotechnology 13 (2002) 5.

[32] J.W. Baldwin, B. Chen, S.C. Street, V.V. Konovaloy, H. Sakurai, T.V. Hughes, C.S. Simpson, M.V. Laxmikantham, M.P. Cava, L.D. Kispert, R.M. Metzger, J. Phys. Chem. B 103 (1999) 4269.

[33] (a) H. Song, C. Lee, Y. Kang, T. Lee, Colloids and Surfaces A: Physiochem. Eng. Aspects 284–285 (2006) 583;
(b) H. Song, H. Lee, T. Lee, J. Am. Chem. Soc. 129 (2007) 3806.

[34] D.E. Gray, American Institute of Physics Hand Book, second ed., McGraw-Hill Book Co., New York, 1963.

[35] H. Likura, S. Mori, M. Sawamura, E. Nakamura, J. Org. Chem. 62 (1997) 7912.

[36] T. Ohno, N. Martin, B. Knight, F. Wudl, T. Suzuki, H. Yu, J. Org. Chem. 61 (1996) 1306.

[37] (a) L.J. Wilson, S. Flanagan, L.P.F. Chibante, J.M. Alford, in: W.E. Billups, M.A. Ciufolini (Eds.), Buckminsterfullerenes, Macmillan, New York, 1993. Chapter 11;
(b) F. Arias, L. Echegoyen, S.R. Wilson, Q. Lu, Q. Lu, J. Am. Chem. Soc. 117 (1995) 1442.

[38] (a) S.H. Yang, C.L. Pettiette, J. Conceicao, O. Chesnovsky, R.E. Smalley, Chem. Phys. Lett. 139 (1987) 233;
(b) M.S. Dresselhaus, G. Dresselhaus, P.C. Eklund, in: Science of Fullerenes and Carbon Nanotubes, Academic Press, 1996, p. 63. Chapter 3.

[39] I.R. Peterson, D. Vuillaume, R.M. Metzger, J. Phys. Chem. A 105 (2001) 4702.